Smartphone Application for Visualizing Building Air Leakage

Philip Boudreaux **Mark Root** **Gurneesh Jatana**

Gina Accawi

ABSTRACT

Annually, unwanted air leakage through building envelopes accounts for 4 quads of energy consumption in the United States, which translates to about 10% of total building energy consumption. Locating and sealing leakage sites is crucial for decreasing building energy consumption. Smartphones are ubiquitous and contain sophisticated cameras and high performance processors that could be employed to visualize air leakage using the background-oriented schlieren imaging technique, making leak detection cheaper and easier. This technique requires a textured and high-contrast background such as a brick or concrete masonry unit wall, a building air leak that has a temperature difference compared with the ambient air, and an imaging system. This work focuses on using smartphones as the imaging system to visualize air leakages. The paper discusses application development and the results of testing to determine leakage visualization performance as a function of leak temperature. The results show that leaks with a temperature difference greater than 16°C compared with the ambient air temperature were visualized using existing smartphones.

INTRODUCTION

Air leakage in buildings wastes 4 quads (1200 TWh) per year in the United States, or about 10% of total building energy consumption (DOE 2014). Locating and sealing leaks is critically important to increasing energy efficiency, reducing energy bills, improving indoor air quality, and maintaining the durability of a building envelope. Typically, a blower door test is used to measure whole building leakage. This test involves installing a fan in a doorway and pressurizing the building, then measuring the flow through the fan. This measured flow is assumed to be equal to the flow through all the leaks in the building. During a blower door test, technicians use infrared thermography, smoke, or simply feel for air currents to locate areas where the building envelope is leaking so that these areas can be sealed (ASTM 2007).

Blower door tests can be time consuming and disruptive to building occupants, but these three detection methods also have their own constraints. Technicians need some training and skill to use infrared thermography to distinguish air leakage

Philip Boudreaux and Gurneesh Jatana are R&D staff members at Oak Ridge National Laboratory, Oak Ridge, Tennessee. Mark Root is a full stack software developer at Oak Ridge National Laboratory, Oak Ridge, Tennessee. Gina Accawi is the group leader of the Research Application Development Group at Oak Ridge National Laboratory, Oak Ridge, Tennessee.

from other thermal anomalies. To help with this task, the direction of the blower door can be switched to complete infrared scanning for both positive and negative pressurization, but doing so is time consuming. Technicians can fill a building with theatrical smoke and then push the smoke out through leaks during pressurization with a blower door, but occupants must be evacuated during this process. Smoke pencils or a hand can be used to methodically check all surfaces of the envelope for leakage, but this technique is tedious and time consuming. The development of a way to locate leakage sites with or without a blower door using a device as ubiquitous as a smartphone will enable widespread leakage detection and sealing by building owners. This work presents a smartphone-based building air leakage detector application that operates based on background-oriented schlieren (BOS) photography.

BACKGROUND

BOS Photography

BOS photography, sometimes called synthetic schlieren, is an optical technique to visualize the flow of transparent fluids that have a different density compared with that of the surrounding fluid (Dalziel et al. 2000). The optical setup is simple; BOS requires only a digital camera and a high-contrast background to visualize a fluid. Because these backgrounds can be manufactured or natural, this technique is uniquely suited for field implementation (Dalziel et al. 2000, Raffel et al. 2000, Hargather and Settles 2009). In contrast, traditional schlieren requires expensive mirrors and complex setups.

BOS is based on Snell's law, which describes the refraction of light as it travels across a transition between two media of different refractive indices (n). Figure 1(a) and Equation 1 describe the refraction of light at the interface of two materials with different refractive indices n_1 and n_2. The variable θ_1 denotes the angle of incidence of the incoming light ray, and θ_2 denotes the angle of refraction of the exiting light ray. For media such as air, the refractive index changes with density according to the Gladstone–Dale relationship, which is shown in Equation 2, where k is the Gladstone–Dale constant, which depends on the wavelength of light and air composition, and ρ is the density of the gas. Density varies depending on temperature T, pressure P, and gas composition (described by the specific gas constant R), as shown in Equation 3.

For imaging building leakage, the temperature difference between leaking and ambient air provides a difference in refractive index. Figure 1(b) shows the optical setup for visualizing air leakage. Equation 4 illustrates the shift of the background image viewed by the camera because of the refraction of the air leakage (Becher et al. 2020). This shift, Δy, is a function of the apparent distance of the leak to the background d_r, the distance between the camera and the background d, the focal length of the camera f, the refractive index of the air leak n, and the refractive index of the ambient air n_0. As d_r increases—that is, as the ratio of the refractive indices increases—the background feature shift Δy also increases.

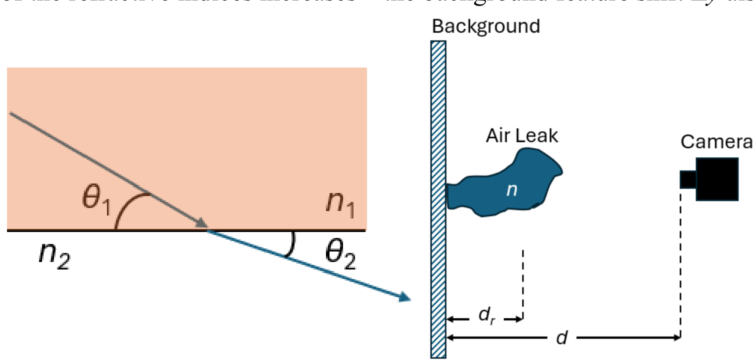

a) b)

Figure 1 (a) An illustration of Snell's law and (b) the optical setup needed to visualize air leakage.

$$\frac{\sin\theta_1}{\sin\theta_2} = \frac{n_2}{n_1} \tag{1}$$

$$(n-1) = k * \rho \tag{2}$$

$$\rho = \frac{P}{R * T} \tag{3}$$

$$\Delta y = \frac{d_r}{d}\left(\frac{fd}{f-d}\right) \cdot 2 \cdot \left(\frac{n}{n_0} - 1\right) \tag{4}$$

Smartphones and BOS

Other studies have shown that smartphones can be used for BOS. Hayasaka and Tagawa (2019) coined the term smartphone BOS (SBOS) and showed that flow visualization results from SBOS are very similar to BOS results and that visualization could be accomplished when the smartphone moved with an observer. Settles (2017) demonstrated that a smartphone with an add-on telephoto lens and offline processing could be used for BOS imaging, noting that better high-speed imaging capabilities and native applications could increase the usefulness of smartphones for BOS. Because no such native application existed, Settles saved high-quality images to memory and then postprocessed them to enable flow visualization. The present work describes the development of a smartphone application called AURA that uses the onboard camera to visualize building air leakage.

Buildings and BOS

Other work has leveraged the convenience of BOS to image air flows in buildings. The authors' previous work used machine vision cameras and open-source software to visualize air flow through building claddings (Boudreaux et al. 2022). Hargather and Settles (2011) used BOS to successfully visualize heating supply vent flow with a temperature difference of 10°C and hot air flow from a wall-mounted passive heat register and a space heater with temperature differences significantly greater than 20°C compared with the ambient temperature. ASTM F1704, *Standard Test Method for Capture and Containment Performance of Commercial Kitchen Exhaust Ventilation Systems*, states that schlieren or shadowgraph methods can be used to determine capture hood spillage (ASTM 2022). Rong et al. (2025) showed that using BOS to determine the capture efficiency of ventilation systems produced results similar to those obtained from tracer gas methods. Herein, the authors expand previous work that used machine vision cameras to the use of smartphones for visualizing building leakage via the custom-built application AURA.

METHODOLOGY

Smartphone Application Development

The authors had three goals for the smartphone application—it should (1) operate on iOS and Android platforms; (2) control key parameters of the phone's camera, including the ISO sensitivity setting, exposure time, and aperture (via camera selection); and (3) process sequential images locally so that flow can be visualized in real time. Thus, AURA, a web-based application, was developed with the option to download and install as a progressive web application (PWA) (Lingolu and Dobbala 2020) so that no cellular or Wi-Fi connection is needed to visualize building leakage. The application uses World Wide Web Consortium standards and guidelines for interacting with a user's camera. Consequently, the application can be accessed using any modern web browser or mobile device such as a smartphone or tablet. It can also be accessed when a user is offline if the PWA version is installed.

Most smartphone camera applications default to automatically controlling gain (ISO) and exposure time to provide casual photographers with suitable pictures. However, scientific imaging demands full control over camera settings, especially those involved in the exposure triangle, a set of three interdependent settings (i.e., ISO, exposure time, and aperture) that impact an image's exposure (how bright it appears). ISO is an amplifier that increases the exposure of an image, but it also introduces noise. For scientific imaging, the ISO value should be kept as low as possible. Exposure time determines how long the sensor is exposed to incoming light. The longer the exposure time, the higher the exposure and brighter the image. The aperture is a physical iris that limits the amount of light that hits the camera's imaging sensor. Most smartphone cameras have a fixed aperture, but the larger the aperture, the brighter the image. Aperture also affects depth of field—that is, the depth of the focal plane. A smaller aperture results in a larger depth of field, whereas a larger aperture results in a shallower depth of field. Visualizing air leakage with a smartphone camera requires keeping ISO as low as possible to reduce noise and using long exposure times to help increase the exposure. Aperture and focal length are typically fixed for each camera available on a smartphone. Therefore, the priority is to select the available camera with the appropriate focal length. For visualizing leakage, a longer focal length typically yields better visualization sensitivity but narrows the field of view. In the current implementation of AURA, ISO and exposure time can be adjusted only on Android devices.

To acquire image data from the camera, AURA uses OpenCV, an open-source computer vision library that provides a wide range of functionality for high-resolution image manipulation (Bradski 2000). OpenCV also has a distribution for web development using WebAssembly, a compilation target for programming languages that enables near-native computing speeds in a browser (Rossberg 2019). Given the computational load needed for AURA and WebAssembly's ability to execute within a mobile browser, OpenCV is a perfect fit for AURA. Using OpenCV to perform the image processing steps described in the following paragraphs, AURA can process 7 megapixel (MP) images at around 2–7 frames per second, which enables real-time leakage visualization.

Figure 2 shows the image processing steps that AURA performs on frames from a camera's video feed to enable leakage visualization using the BOS technique. First, after the camera settings are chosen, a video feed (composed of frames, or images) of a leak in front of a high-contrast background streams from the camera to AURA. After an image (I) is converted to grayscale, AURA performs a pixel-by-pixel subtraction of the previous frame in the stream (I_{i-1}) from the current frame (I_i), producing an image that consists of only differences in intensity for each frame. These differences in intensity are caused by random electronic noise and the schlieren effect described in the section on "BOS Photography." In Figure 2, the resulting difference image is black. The histogram below the black image shows that all pixels have an 8-bit intensity value of less than 30; most have a value less than 4.

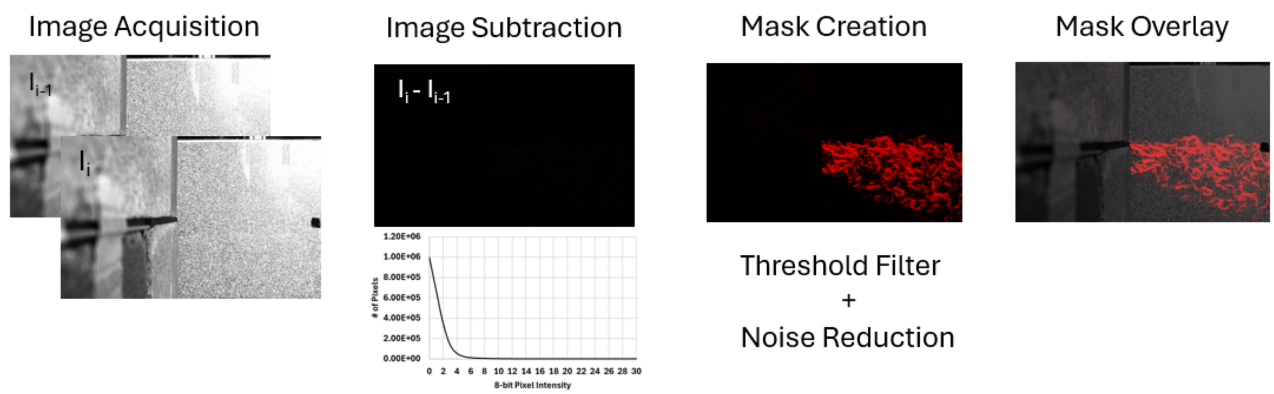

Figure 2 AURA processing steps for visualizing air leakage from sequential frames from a smartphone camera video feed.

To visualize such a weak signal, a mask is created using a two-step process. First, all pixels with an intensity greater than a user-selected value (in this example, 5) are set to 1 in a binary matrix with the same resolution as that of the original frame. All pixels less than this threshold are set to 0. A red color mask is then applied to the binary matrix. Second, users can denoise the resulting mask to reduce random electronic noise in the image. A median blur noise filter is used to change pixels in the binary mask from 1 to 0 if they do not have sufficient neighboring pixels with a value of 1. Finally, the mask is overlaid on the original image from the camera so users can visualize the location of the leak in real time. Figure 3 shows screenshots of AURA 0.2.7 beta on an Android-based smartphone. Figure 3(a) shows the welcome screen. By selecting "Air Leak Detection" on the welcome screen, users can select the camera [Figure 3(b)] and processing settings such as threshold pixel intensity, noise filter, and how much the original image should be darkened under the mask (Figure 3[c]). On the

Android platform, users can also select camera settings such as zoom, focus distance, ISO, exposure time, and white balance. Focus distance, ISO, exposure time, and white balance are not yet available on iOS devices.

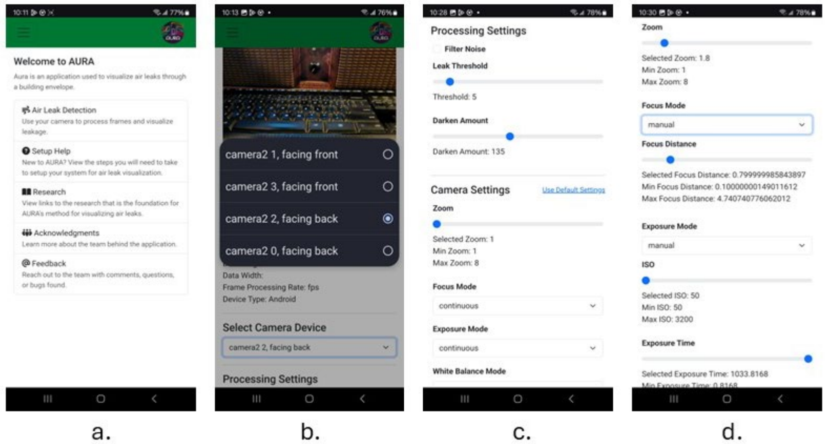

Figure 3 AURA screen shots: (a) welcome screen, (b) camera selection, (c) processing settings, and (d) camera settings.

Experimental Setup

A series of experiments was conducted to test AURA's performance on two phones, an iPhone 15 and a Samsung Galaxy S22 Ultra. Table 1 shows the camera specifications and AURA settings used on each smartphone. At the time of this writing, manual cameras are available only on the Samsung smartphone. Experiments were conducted with various temperature differences between the air leak and the ambient air to determine the lower temperature detection limit of the AURA detector.

Table 1: Camera Specifications and Settings for Experimental Tests

Smartphone	Focal Length, mm (in.)	Aperture, *f*	ISO	Exposure Time (ms)	Focus, m (in.)
iPhone 15	26 (1.02)	1.6	Auto	Auto	Auto
Samsung Galaxy S22 Ultra	23 (0.91)	1.8	50	103	0.809 (31.9)

Figure 4 shows the experimental setup used to test the phones. Figure 4(a) shows a schematic of the system used to create a controlled hot air leak. The system consisted of compressed air fed into a pressure regulator (to set the desired flow rate), a Bronkhorst Mass-Stream D-6360-DR flow meter, and an Omega AHP-5052 inline AC heater controlled by a variable 120 V transformer. The leak temperature was measured at the outlet of a short section of flexible tubing connected to the end of the heater using an Omega P-M-1/10-1/8-6-0-T-3 resistive temperature device (RTD) and compared with the ambient air temperature, which was also measured with an RTD. The leak was centrally placed between the smartphone and background, which were 32 in. (0.81 m) apart. Figure 4(b) shows the optical setup and indicates the locations of the background, leak, smartphone, and Genaray Full Moon LED light used for ambient lighting. While AURA was running and visualizing the leak, the built-in screen recorder function of each smartphone was used to capture AURA's visualization screen.

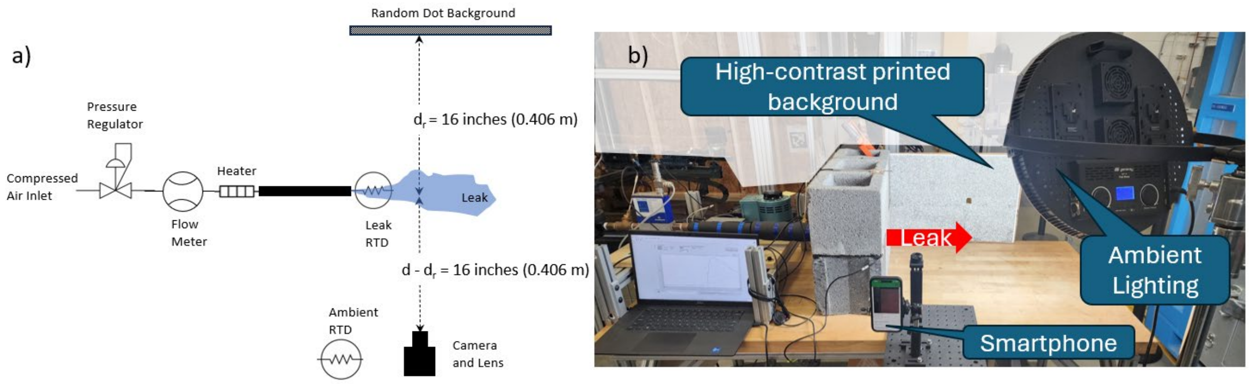

Figure 4 (a) Schematic of system used to create a hot air leak, with controls for flow rate and temperature and (b) experimental setup with smartphone, background, and ambient lighting.

RESULTS AND DISCUSSION

Data were acquired at leak-to-ambient temperature differences of 22°C (40°F), 19°C (34°F), 16°C (29°F), 13°C (23°F), and 11°C (20°F) for each smartphone using the AURA application with the cameras and settings shown in Table 1 and the experimental setup shown in Figure 4. The leakage flow rate was 1 ft^3/min (0.0005 m^3/s) with a velocity of 730 ft/min (3.7 m/s). This leak velocity is between the velocity expected when pressurizing the building to 50 Pa and the velocity under normal stack effect in the winter which is approximately 1 m/s. The results for each smartphone are shown in Figure 5. The first image for each phone shows a cropped view of the high-contrast random dot background imaged by the camera. The subsequent images show the leakage visualizations at various temperature differences. Because AURA does not yet support manual camera control on iOS devices, the camera was used in automatic mode on the iPhone, which sets focus distance, ISO, exposure time, and white balance automatically.

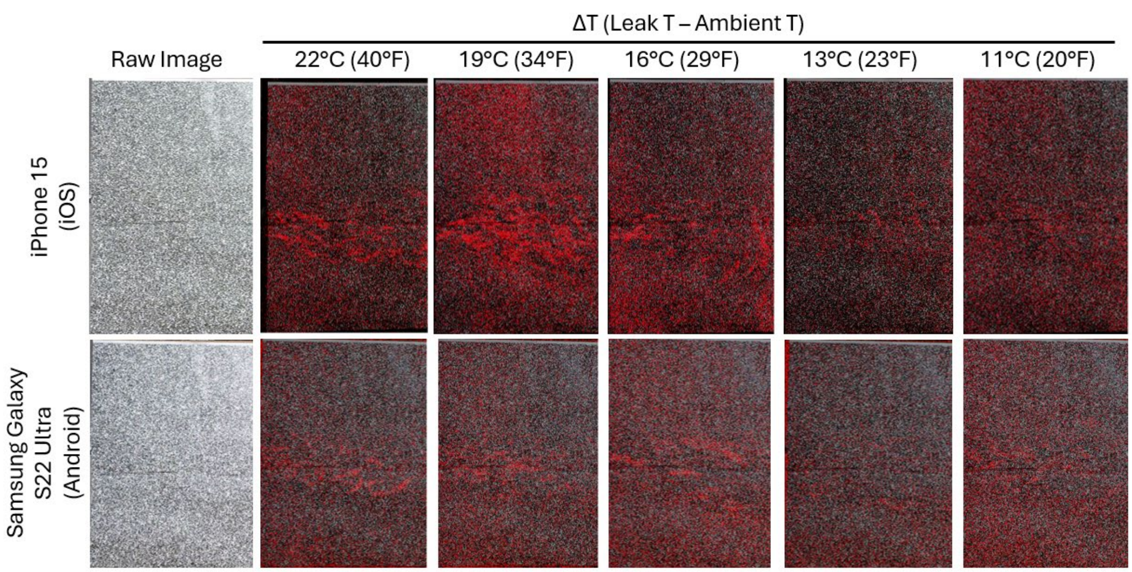

Figure 5 AURA leakage visualizations of temperature differences greater than or equal to 16°C (29°F) for two phones and six leak-to-ambient-temperature differences.

The Android phone was not able to visualize the flow when the camera was in automatic mode, so the camera settings were changed to those reported in Table 1. Even when the Android device used these optimized settings, the iOS device more clearly visualized the leak. However, both smartphones were able to visualize leakage with a temperature difference of 16°C (29°F) or greater. Determining why the iPhone 15 performed better than the Samsung Galaxy S22 Ultra is difficult. The iPhone and Samsung smartphone cameras have similar specifications, binning very small pixels to create 12 MP images with equivalent pixel sizes of 2.44 µm (0.096 mil) and 2.4 µm (0.094 mil), respectively. On iOS and Android devices, the images processed in AURA are smaller than the originals (2160 × 3280 pixels or 7.1 MP). Differences in visualization performance may be due to differences in image processing carried out by the phones before the images are passed to AURA's OpenCV code.

Required Temperature Difference for Building Leakage Visualization

Figure 5 shows that with an ideal optical setup and background contrast, the AURA smartphone application can visualize leakage with a temperature difference of 16°C (29°F) or more from the ambient temperature. In the field, the background behind a leak and the optical setup will be less than ideal, so performance is likely to suffer. This issue is discussed in the next section. Detecting leaks with a temperature difference of 16°C or more compared with ambient temperatures limits the time of year during which leaks can be found. Figure 6 shows the times of the year when ΔT is greater than or equal to 16°C (29°F) and 10°C (18°F) for each climate zone in the US during the workday (7 a.m.–6 p.m.). A minimum detection limit of 10°C (18°F) more than doubles AURA's working hours per year in hot and mixed climates. Previous work showed that a more expensive machine vision camera, with better imaging performance than that of a smartphone camera, can visualize leakage with temperature differences as low as 10°C (18°F) (Boudreaux et al. 2025).

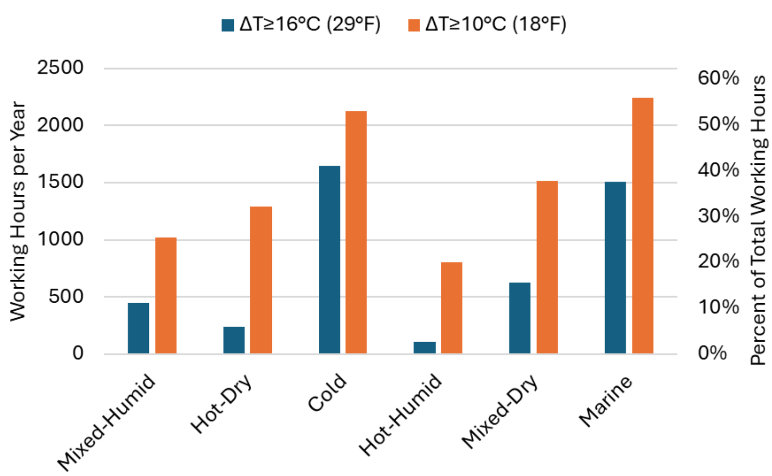

Figure 6 Times of year when a BOS-based air leakage detector can be used based on a ΔT detection limit.

Required Optical Setup Constraints for Building Leakage Visualization

As mentioned previously, two constraints on visualizing building leakage may make the in-field detection limit higher than 16°C. First, because building leakage emanates from a background (i.e., building cladding or an indoor surface), the ratio d_r/d described in Equation 4 is smaller than the ratio for the experimental setup shown in Figure 4. This paper presents results for a d_r/d ratio of 0.5. According to Equation 4, the larger the ratio, the larger the pixel shift and the easier it is to visualize leakage. When visualizing leaks in the field, the camera can be brought closer to the background to increase the d_r/d ratio and improve visualization. However, this approach reduces the camera's field of view, which makes locating leaks more time consuming. Visualizing leaks through a concrete masonry unit wall with a low d_r/d ratio was investigated in greater detail in a previous paper. Boudreaux et al. (2025) showed that the best visualization occurred when the machine vision camera's optical axis was normal to the building surface; in this optical setup, leaks were visualized with temperature differences as low as 10°C (18°F)

Required Background Contrast Constraints for Building Leakage Visualization

A further limitation when using BOS-based leak detection for building leakage is that many surfaces do not have high contrast. A high-contrast background is needed for BOS imaging because the method detects shifts of background textural features, such as the shift in the position of a dot on the random dot background, imaged on the camera sensor. If a background (e.g., a solid white interior wall) has no features that can shift, then leakage cannot be visualized. This limitation can be remedied by projecting a high-contrast pattern on any building surface. Using the optical setup shown in Figure 4, the authors used AURA running on the iPhone 15 to visualize a leak with a 22°C (40°F) temperature difference in front of a piece of white drywall, without and with background projection. Figure 7 shows the test setup and visualization results. The flow could not be visualized in front of the drywall without the background projection (Figure 7[b]), but the flow was visualized when the background projection was used (Figure 7[c]). A LumiBlazeR LED pattern projector (Innovations in Optics, Inc.) with a point cloud reticle was used to project a high-contrast point cloud pattern on the drywall. In the field, an affordable laser pointer and diffuser could be used to create sufficient contrast on any surface. An affordable laser pointer and diffuser could be used to create sufficient contrast on any surface in the field.

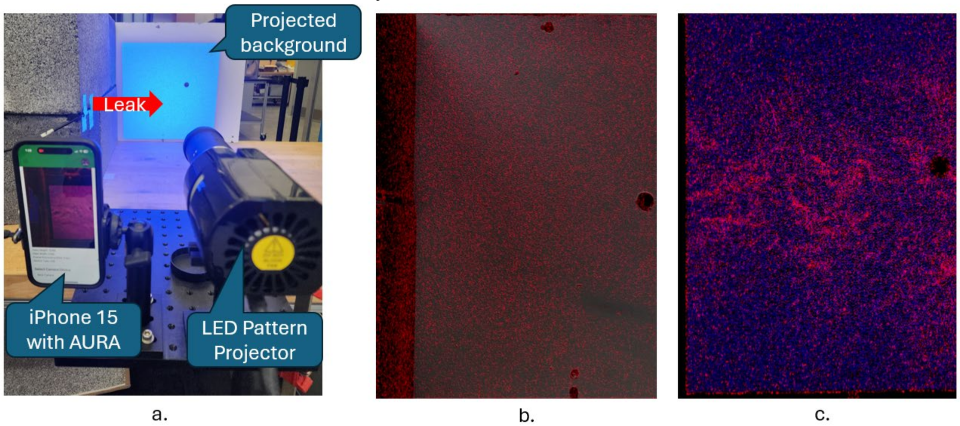

Figure 7 Visualizing leaks with a drywall background and a projected high-contrast pattern: (a) experimental setup, (b) AURA results without pattern projection, and (c) AURA results with pattern projection.

CONCLUSIONS

A smartphone application called AURA that uses integrated cameras to visualize building leakage was developed to better enable building air leakage detection and sealing to reduce building energy consumption. AURA's real-time visualization relies on BOS imaging and a new, fast method for visualizing BOS imaging signals. Initial testing showed that the beta version of AURA can visualize leaks with temperature differences as low as 16°C (29°F) compared with ambient temperatures. Increasing the image resolution that AURA processes and optimizing camera settings could further decrease this minimum detection limit.

ACKNOWLEDGMENTS

This article and the work described herein were sponsored by the US Department of Energy (DOE) Building Technologies Office. Special thanks to Sven Mumme and Marc LaFrance, DOE technology managers, for their leadership in this project. The authors also thank Oak Ridge National Laboratory staff members Hayden Esser and Abby Barnes for help with AURA development.

REFERENCES

ASTM. 2017. ASTM E1186-17, *Standard Practices for Air Leakage Site Detection in Building Envelopes and Air Barrier Systems*. Philadelphia, PA: ASTM.

ASTM. 2022. ASTM F1704, *Standard Test Method for Capture and Containment Performance of Commercial Kitchen Exhaust Ventilation Systems.* Philadelphia, PA: ASTM.

Becher, L., C. Voelker, V. Rodehorst, and M. Kuhne. 2020. Background-oriented schlieren technique for two-dimensional visualization of convective indoor air flows. *Optics and Lasers in Engineering* 134:106282.

Boudreaux, P., S. Ventkatakrishnan, E. Iffa, and D. Hun. 2022. Application of reference-free natural background–oriented schlieren photography for visualizing leakage sites in building walls. *Building and Environment* 223:109529.

Boudreaux, P., S. Killough, R. Zhang, G. Jatana, and D. Hun. 2025. Development of novel techniques for non-invasive air leakage and moisture detection in building envelopes. *ASHRAE Transactions* 131(1):131–139.

Bradski, G. 2000. The OpenCV Library. *Dr. Dobb's Journal of Software Tools* 120:122–125.

Dalziel, S. B., G. O. Hughes, and B. R. Sutherland. 2000. Whole-density density measurements by 'synthetic schlieren.' *Experiments in Fluids* 28:322–335.

DOE. 2014. *R&D Roadmap for Emerging Window and Building Envelope Technologies*. Washington, DC: US Department of Energy.

Hargather, M. J., and G. S. Settles. 2009. Natural-background-oriented schlieren imaging. *Experiments in Fluids* 48:59–68.

Hargather, M. J., and G. S. Settles. 2011. Background-oriented schlieren visualization of heating and ventilation flows: HVAC-BOS. *HVAC&R Research*. 17(5):771–780.

Hayasaka, K., and Y. Tagawa. 2019. Mobile visualization of density fields using smartphone background-oriented schlieren. *Experiments in Fluids*. 60:171.

Lingolu, M., and M. Dobbala. 2020. A comprehensive review of progressive web apps: Bridging the gap between web and native experiences. *International Journal of Science and Research*. 11(2):1326–1334.

Raffel, M., H. Richard, and G. E. A. Meier. 2000. On the applicability of background oriented optical tomography for large aerodynamic investigations. *Experiments in Fluids* 28:477–481.

Rong. J., Y. Huang, Y. Zhao, et al. 2025. A novel measurement for evaluating the capture efficiency of local ventilation system using background oriented schlieren. *Building and Environment*. 267:112185.

Rossberg, A., ed. 2019. WebAssembly Core Specification. W3C. https://www.w3.org/TR/wasm-core-1/.

Settles, G.S. 2017. Smartphone schlieren and shadowgraph imaging. *Optics and Lasers in Engineering* 104:9–21.